S-Parameter Measurements and Microwave Applications of Superconducting Flux Flow Transistors

J. S. Martens, Vincent M. Hietala, *Member*, *IEEE*, Thomas E. Zipperian, *Member*, *IEEE*, D. S. Ginley, Chris P. Tigges, and Julia M. Phillips

Abstract—**We have performed microwave two-port *S*-parameter measurements and modeling on superconducting flux flow transistors. These transistors, based on the magnetic control of flux flow in an array of high temperature superconducting weak links, can exhibit significant available power gain at microwave frequencies (over 20 dB at 7–10 GHz in some devices). The input impedance is largely inductive while the output impedance is both resistive and inductive. The characteristics are such that these devices are useful in numerous applications including matched amplifiers, phase shifters and active impedance convertors.**

Introduction

THE SUPERCONDUCTING flux flow transistor (SFFT) is a relatively recently developed active four terminal superconducting device (e.g., [1]–[5]). The objective in its development was to produce a very fast device fabricated from high temperature superconducting (HTS) materials that required only a single superconducting film. The device exhibits high speed operation (10–30 ps transit times with 3 μm minimum feature size), large gain and impedance levels that are suitable for many applications. The present work concentrates on small signal *S*-parameter measurements of these devices at 77 K (made of $YBa_2Cu_3O_7$ and of $Tl_2Ca_2Ba_2Cu_3O_{10}$), noise measurements, and a discussion of two SFFT applications (amplifier and phase shifter) that can be better modeled employing these data.

Device Basics

The typical SFFT consists of a parallel array of weak superconducting links connecting two unweakened superconducting electrodes and a superconducting control line near the links to provide a local magnetic field. An example of this structure is shown in Fig. 1; ground is that of a coplanar waveguide structure (not shown) surrounding the device for efficient coupling. The links are typically 2–3 μm wide by 10 μm long, separated by 6 μm and 50–90 nm thick (while the electrodes are at least 200 nm thick). The localized thickness reduction is important to allow flux flow in a well-defined path. This maximizes flux speed and keeps the voltage levels reasonable (1–100 mV in normal operation). The number of links does not strongly affect performance but larger numbers of links help by lowering output resistance and slightly increasing device gain at the expense of frequency response [5]. When the device is biased below the critical current of the link region, typically 0.5–5.0 mA, no flux is admitted into the link system (perfect Meissner state). Above the critical current, flux is admitted in discrete quanta known as vortices [6]. These vortices can move due to the 'Lorentz' force generated by the bias current. Other forces affecting the vortex motion are pinning (probably not present to any significant extent in the Tl materials at 77 K but can possibly be a problem in YBaCuO), effective viscosity of the superconductor, external magnetic fields from the control line or parasitic sources, and surface barriers that hamper the motion of flux into and out of the links. Many of these forces are functions of the superconductor quality and thus emphasize the importance of good film growth. The balance of all of these forces determines the flux motion and hence the terminal voltage via Faraday's law. In terms of active device perfor-

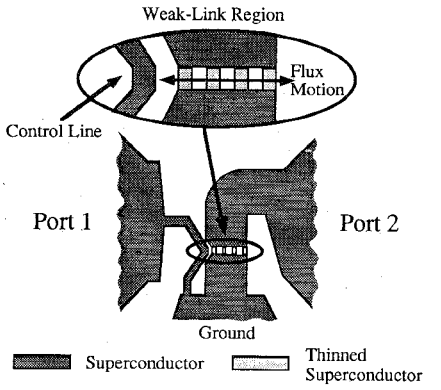

Fig. 1. Layout of the superconducting flux flow transistor. Port 1 is the control line and port 2 is the device body.

Manuscript received March 28, 1991; revised July 8, 1991. This work was supported by the U.S. Department of Energy through Sandia National Laboratories under contract No. DE-AC04-76P00789.

J. S. Martens, V. M. Hietala, T. E. Zipperian, D. S. Ginley, and C. P. Tigges are with Sandia National Laboratories, Department 1140, Albuquerque, NM 87185.

J. M. Phillips is with AT&T Bell Laboratories, 600 Mountain Avenue, Murray Hill, NJ 07974.

IEEE Log Number 9102784.

mance, the key principle is the use of the external magnetic field from the control line (the input) to modulate the flux density and flux motion in the link system [7], [8] and consequently the resulting output characteristics.

Devices have been made from films of TlCaBaCuO and YBaCuO on $LaAlO_3$ substrates. The TlCaBaCuO samples were made by sequential *e*-beam evaporation of the elements followed by sintering in air (typically 16 min at 850 C) under a partial pressure of Tl-O and annealing in oxygen (typically 10 min at 750 C) as described in detail elsewhere [9]. The films show complete *c*-axis orientation normal to the substrate and are primarily *a*-axis oriented in the plane as well. Grain sizes are typically larger than 100 μm, film thicknesses were nominally 300 nm, the films are smooth on a scale < 50 nm and the phase is predominantly 2223. The Tl samples used in these experiments had T_c's of about 103 K and critical current densities at 77 K (0 field) of about 350 kA/cm^2. In making the YBaCuO films, Y and Cu metals are evaporated from separate electron gun sources and BaF_2 is resistively evaporated [10]. Composition ratios of Y:Ba:Cu of 1:2:3 within 1% were confirmed [11]. The YBaCuO films are nominally 200 nm thick and are epitaxially oriented with the *c*-axis normal to the substrate. The samples are annealed *ex situ* in a carefully optimized multi-stage process [12] to produce T_c's of about 90 K and critical current densities at 77 K (0 field) of about 1 MA/cm^2. While pinning may be significant in some *in situ* grown YBaCuO films, those films used in these experiments had much lower pinning and hence are more likely to make good SFFT's (high flux speed and hence low transit time) [12].

The devices and associated circuitry are formed with standard optical lithography and etched with a 2% Br in isopropanol solution. The etch rate varies between HTS materials and between different stoichiometries (a sample off-stoichiometry by 5% may etch at half the speed of its on-stoichiometry counterpart). The links are thinned with respect to the body in a separate photolithographical step that leaves a window open over the active region. The links are exposed to a 0.5% Br in isopropanol solution iteratively until the I-V curves (at 77 K) reach the desired form (usually a given transresistance range). Contacts (annealed Ag), interlevel dielectrics and normal metal overlays are deposited and patterned by standard microelectronic techniques.

I-V curves for two of the devices (one made of TlCaBaCuO and one of YBaCuO) are shown in Fig. 2. The current through the link system (or body) is denoted by I_{bdy} while the control current is labeled I_{ctl}, the voltage across the body terminals will be labeled throughout as V. The two most important circuit parameters to be obtained from these curves are the transresistance ($r_m = \Delta V/\Delta I_{\text{ctl}}$) and output resistance ($r_o = \Delta V/\Delta I_{\text{bdy}}$). For the microwave measurements, the devices will be biased $I_{\text{bdy}} = 8$ mA and $I_{\text{ctl}} = 0.2$ mA where typical values are $r_m \approx 17$–$19\ \Omega$ and $r_o \approx 3$–$4\ \Omega$. An equivalent circuit based on device physics is shown in Fig. 3 [5]. Since moving flux generates a voltage and the control variable is

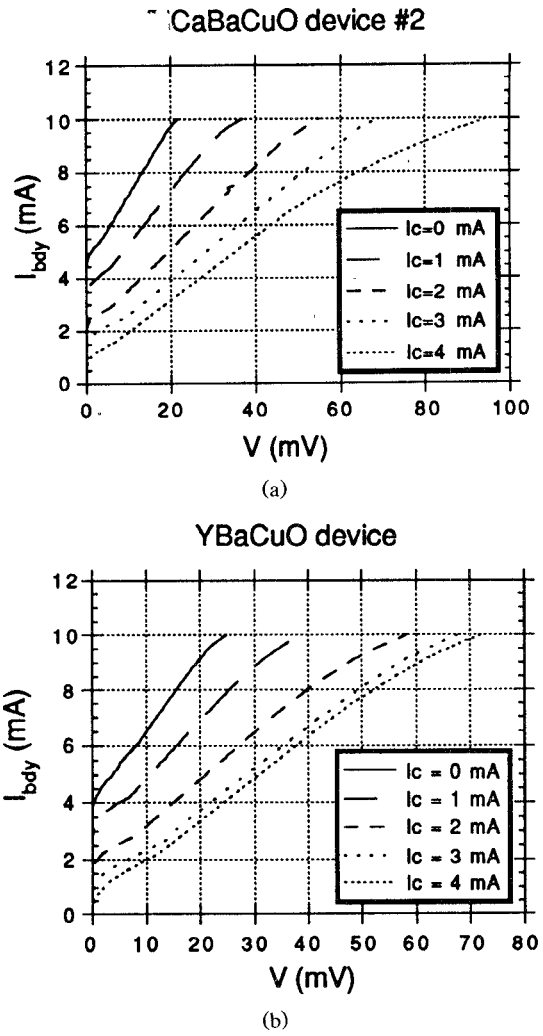

Fig. 2. IV curves of two SFFT's. (a) TlCaBaCuO device. (b) YBaCuO device. I_{bdy} is the current through the device body (link region) and I_c is the control current. The voltage V is measured across the link system.

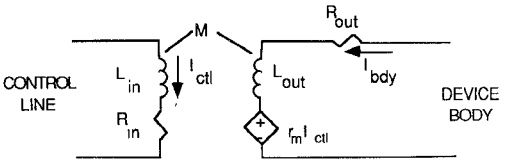

Fig. 3. Equivalent circuit of the SFFT. Values of the components are discussed in the text. The transresistance component is the active element. Other interesting features include the nonlinearity of the output inductor and the low amount of cross-talk (M is typically 10 pH).

a current, a transresistance is the active element for the equivalent circuit. The moving vortices have normal cores and hence represent an ohmic resistance (r_o). The input and output impedances are both inductive because of the geometry of the structures and, for the output inductance, because of the excess kinetic inductance of the thin superconducting film in the link region [13]. Since the output inductance (kinetic portion) and output resistance are affected by the number of vortices in the links, these two parameters will be functions of bias. Since $I_{\text{ctl,dc}}$ and $I_{\text{bdy,dc}}$ affect the ability to nucleate more vortices with an

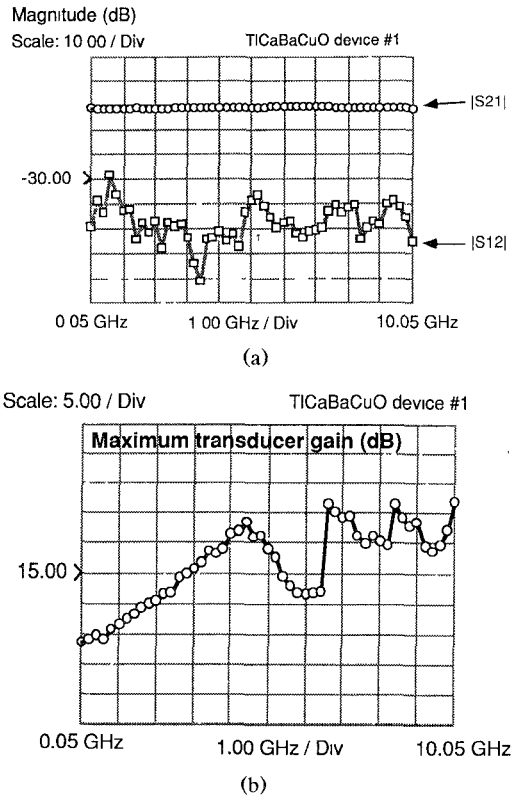

Fig. 4. Measured S-parameters (a) and computed maximum transducer gain (MTG) (b) for a Tl SFFT probed with Cascade signal-ground probes. Note the low $|S_{12}|$ and large available gain. The roughness of MTG is due to contacting problems. For all MTG plots, maximum available gain is used when the device is stable and maximum stable gain is used otherwise.

external field and affect vortex transport properties, r_m is also a function of bias. The small input resistance (≈ 0.1 Ω) arises from contact resistance and surface resistance of the control line.

S-Parameter Measurements

The first measurements were made with Cascade Microtech signal-ground probes using SOLT (short, open, load, thru) calibration [14]. This probing scheme presented problems because of planarity requirements and the irregularity of the $LaAlO_3$ substrates used. As a result, contacting was difficult. Data were obtained for one Tl device at 77 K with some effort and these results are summarized in Fig. 4. The maximum transducer gain (MTG) [15] shown in Fig. 4 is defined as maximum stable gain when the device would be potentially unstable. The roughness of the MTG is due largely to unstable contacts (particularly in the liquid nitrogen environment). There are, however, some interesting features of these data. S_{21} is reasonably large in magnitude and $|S_{21}| \gg |S_{12}|$, indicating active behavior. The measurement of these two parameters was relatively repeatable (to within ≈ 1 dB) and at least semi-quantitatively correct since an unbiased device showed $|S_{12}| = |S_{21}| \approx -40$ dB across the band. The MTG, while having some uncertainty, does indicate the possibility of large gain with adequate matching.

Custom probes using Cascade Microtech mounts and spring-loaded pogo launchers in a ground-signal-ground configuration were designed to circumvent contacting problems. These probes, though still not perfected, did allow for highly repeatable measurements below 10 GHz. Dual-band TRL (thru, short, delay) calibration [14] at 77 K was employed. The 77 K S-parameters for the two devices (whose IV curves are in Fig. 2) are shown in Fig. 5. The bias point ($I_{bdy} = 8$ mA, $I_c = 0.2$ mA) was chosen because r_m was nearing its plateau value and r_o was still relatively small. S_{21} behaves as with the device of Fig. 4 but $|S_{12}|$ is larger. This is largely due to poor isolation with the present probe design. To verify the isolation problem, both probes were placed on a shorting block about the same distance apart from each other as during the transistor measurement and the S-parameters were measured. The measured $|S_{12}|$ and $|S_{21}|$ are shown in Fig. 6 and indicate the poor isolation which is undoubtedly masking the true transistor S_{12}. The actual device S_{12} is probably like that shown in Fig. 4. MTG calculations are shown in Fig. 7 (using the actual measured device data). Even with the S_{12} error, the MTG exceeds 14 dB. We expect that 20–25 dB is closer to the actual MTG over this band. The stability factor K is included in these plots indicating where the gain definitions change and suggesting that the SFFT can be used as an oscillator as has been demonstrated [16].

Model parameters can be determined by fitting the equivalent circuit to the data of Fig. 5. After removing launch parasitics (obtained by looking at a device electrode configuration with no SFFT in place), the equivalent circuit of Fig. 3 was fit to the data for the YBaCuO device of Fig. 5(b). The control line was found to be adequately modeled by a 0.3 nH input inductance and an input resistance of 0.2 Ω at all bias points. With a bias of $I_{bdy} = 8$ mA and $I_c = 0.2$ mA, the other model parameters for the YBaCuO device were $r_m \approx 18.2$ Ω, $r_o = 3.7$ Ω and $L_{out} \approx 0.17$ nH. The fitting process was repeated for the TlCaBaCuO device for a variety of bias conditions and the results are shown in Table I. As is apparent, the output resistance, transresistance, and output inductance are all reasonably strong functions of bias. The transresistance reaches a relatively broad plateau while the output resistance and inductance are somewhat more volatile. The dependence of the output inductance on control current is suitable for phase shifting. The effect of changing control current is qualitatively similar to that of changing the body current since in both cases local fields are being modified. The quantitative changes are different because of the control field anisotropy and screening currents generated.

The effect on parameter values of the material family used is difficult to ascertain because of varying film quality. The penetration depths of the YBCO and Tl films were comparable. Hence for links of the same thickness, the inductance profiles should be similar [13]. This was indeed observed. The quality of the superconductor near the interface with the substrate will strongly affect trans-

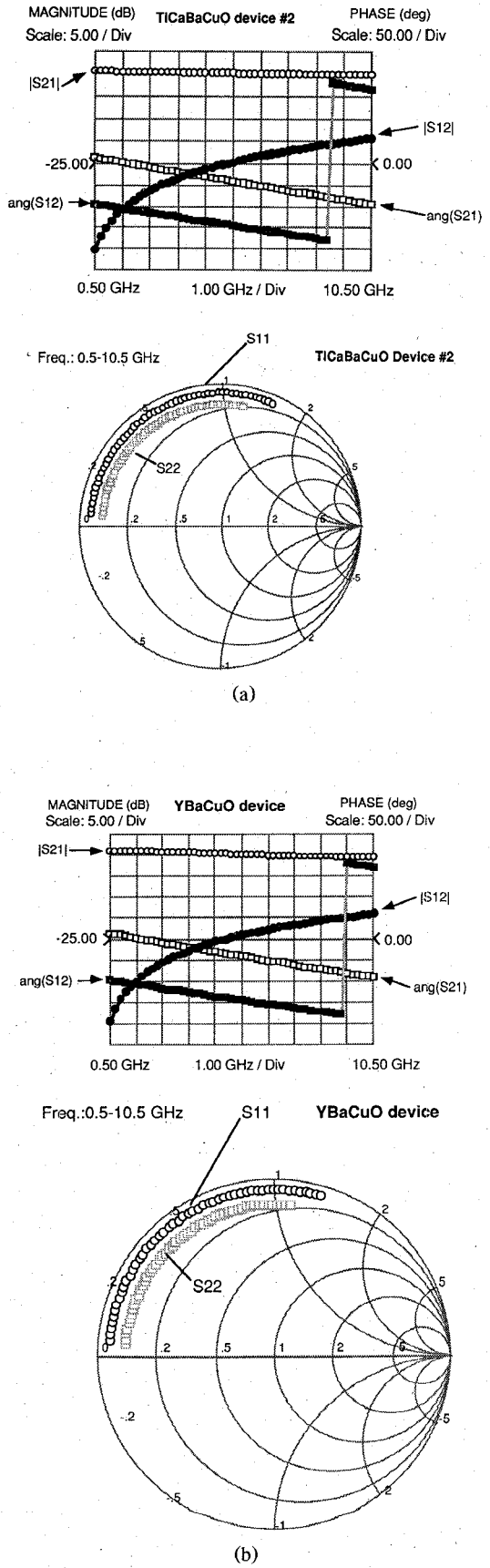

Fig. 5. Measured *S*-parameters of a TlCaBaCuO device (a) and a YBaCuO device (b) both probed using spring-loaded probes for better contact. In both cases, the bias conditions were $I_{bdy} = 8.0$ mA and $I_c = 0.2$ mA. The data show inductive input and output impedances (low in magnitude) and a higher $|S_{21}|$ due largely to the probes.

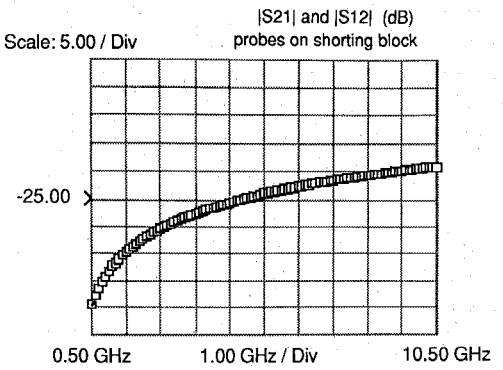

Fig. 6. Measured $|S_{21}|$ and $|S_{12}|$ of the two probes (spring-loaded) placed on a shorting block separated by the spacing used in the Fig. 5 experiments. This shows that the true $|S_{12}|$ of the devices is probably no higher than that shown in Fig. 4.

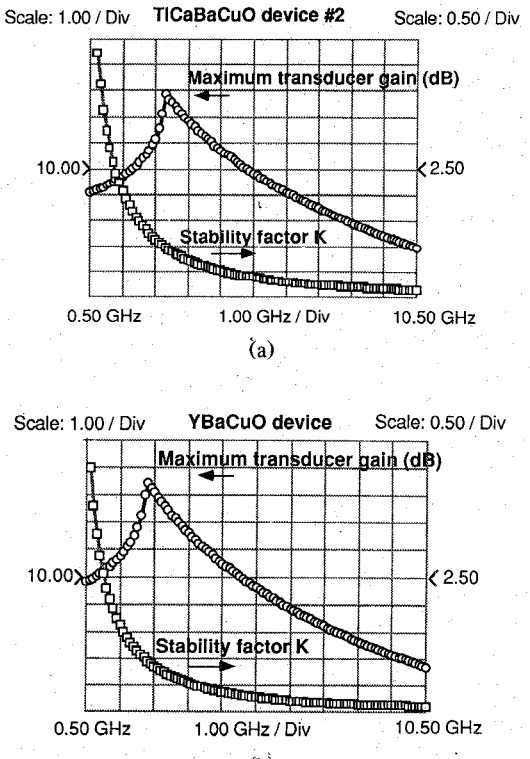

Fig. 7. Computed maximum transducer gain and stability factor K of the devices measured for Fig. 5. (a) TlCaBaCuO device and (b) YBaCuO device. Even with the error in S_{12}, the MAG exceeds 13 dB.

TABLE I
EQUIVALENT CIRCUIT PARAMETER VALUES FOR THE DEVICE OF FIG. 5(a) AT VARIOUS BIAS LEVELS

TlCaBaCuO Device #2						
I_{bdy}(mA)	I_c(mA)	$r_m(\Omega)$	$r_o(\Omega)$	L_{out}(nH)	L_{in}(nH)	$R_{in}(\Omega)$
6.0	0.2	10.2	3.9	0.65	0.3	0.1
8.0	0.2	17.8	4.0	0.49	0.3	0.1
10.0	0.2	18.0	4.5	0.32	0.3	0.1
6.0	2.5	6.8	9.3	0.30	0.3	0.1
8.0	2.5	8.8	9.7	0.18	0.3	0.1
10.0	2.5	9.2	10.1	0.1	0.3	0.1

Note the variability of the output inductance and resistance and the plateau that r_m quickly reaches.

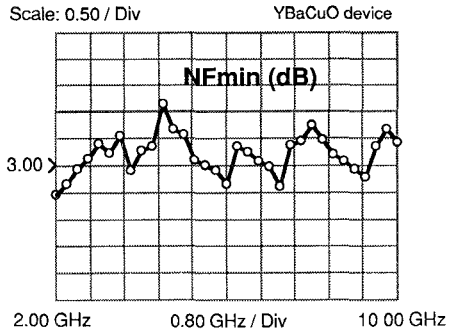

Fig. 8. Minimum noise figure of the YBaCuO device of Fig. 5(b). The results are consistent with a system dominated by flux noise.

resistance and output resistance since the links are very thin. The YBaCuO films have been shown to have very good interfaces, hence it is not surprising that the output resistances are a bit lower for equal link thicknesses as seen by comparing the above YBaCuO model parameters to those for TlCaBaCuO shown in Table I. Little difference is seen in transresistance since each device was tuned (links thinned iteratively) to produce roughly the same transresistance. Although not generally true because of differences in pinning and critical fields, in this case the link thicknesses were roughly equal as well.

Within a given material family and using the same device design, the model parameters seem to be representative. Two YBaCuO devices have been fully characterized and their parameters are within 15%. Five TlCaBaCuO devices have been fully characterized and their parameters fit are within 20% of each other.

Noise Performance

Noise parameters of SFFTs have been measured using Cascade Microtech noise test set from 2–10 GHz. The spring-loaded pogo launchers were again used for probing. The computed minimum noise figure is shown in Fig. 8 for the bias state ($I_c = 0.2$ mA, $I_{bdy} = 8.0$ mA). The value of NF_{min} averages about 3 dB across the band with excursions between 2.5 and about 4.2 dB. Flux noise, a process analogous to shot noise, seems to be the dominant noise source. Calculations of flux noise based on a doubly stochastic Poisson process (the events being the entry of vortices into a link and how closely they bundled with other vortices) produced noise figures in the 2–6 dB range depending on assumptions about the vortex generation process [17]. The noise figures are fairly large since the quantum in this case, a vortex, is physically much larger than an electron (the quantum in conventional electronics). Noise circles are shown in Fig. 9 for the YBaCuO device at 5.0 GHz. The optimal match is near the conjugate of the input impedance as is expected for a nearly unilateral device. The noise figure is not very sensitive to source impedance at any of the frequencies tested for this device. Work continues on reducing the noise levels by improving material quality (to increase the coherence of the flux motion) and by changing the design

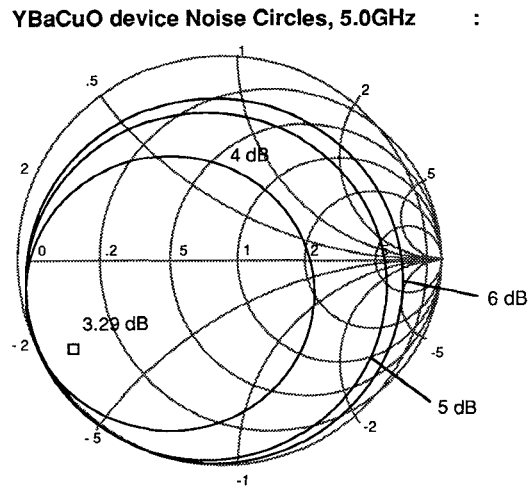

Fig. 9. Noise circles for the YBaCuO device of Fig. 5b at 5.0 GHz. The noise figure in dB is indicated on the circles. The optimum source impedance is close to the conjugate match as would be expected for a nearly unilateral device.

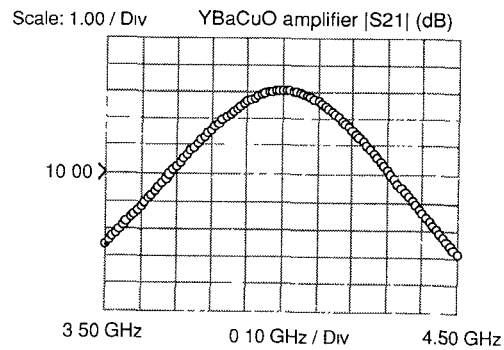

Fig. 10. Performance of a matched amplifier constructed with the device of Fig. 5(b). Maximum gain of 13 dB was achieved with a bandwidth of almost 1 GHz.

of the link system (to improve the flux entry and exit processes).

Applications

As indicated by the MTG calculations shown in Figs. 4 and 7, a matched amplifier should exhibit very high gain [4]. The most recent results are shown in Fig. 10 using the device of Fig. 5(b). A maximum gain of about 13 dB was achieved with an input return loss of ≈ 9 dB at midband (on the order of what can be achieved with a single MESFET). The matching attempt was not to achieve MTG, but rather to maximize gain while maintaining a 1 GHz bandwidth at a center frequency of 4 GHz. The matching in this case was done with normal transmission line sections for convenience, but superconducting matching networks which have insertion loss advantages have been used previously [4]. Since the impedance mismatch is rather severe, relatively high currents will be flowing on the device side of the matching net and any normal conductor losses will become significant.

Another application of interest is a quasi-distributed phase shifter that utilizes the variable output inductance

of the SFFT discussed earlier and demonstrated in Table I. The structure is shown in Fig. 11 [18] and is analogous to the synthetic transmission line structure used for varactor-based phase shifters in that the variable reactance of a component in a semi-lumped transmission line is used to controllably alter the phase velocity of the line. In this case, the control current is changed causing L_{out} and hence the phase velocity of the line to change. The actual test structure is 1 cm long, consists of 12 devices (with a control line separation of 6 μm) separated by 0.5 mm and has a maximum differential electrical length (maintaining phase shift linearity) of 3π at 5 GHz. The capacitances (typically 0.5–0.6 pF) are formed from very short, low impedance sections of the transmission line as shown. Reasonable bandwidth is possible since the quasi-distributed structure maintains impedance levels over an extended frequency range. The phase shift as a function of control current (at 5.0 GHz) is shown in Fig. 12(a) for a YBaCuO circuit. About 2π of phase shift is available with 2.5 mA of control current. Insertion loss is a major concern and a plot of $|S_{21}|$ as a function of control current at 5.0 GHz is shown in Fig. 12(b). With 2π of phase shift, the insertion loss is about 2.1 dB which is certainly competitive with many discrete shifters. The key to successful SFFT phase shifters is the ability to make the links very thin (< 40 nm) so that the kinetic inductance contributions are high. This requires epitaxial films with extremely thin interface layers (which cannot be neglected in HTS because of the large lattice mismatches and unusual chemistry involved). As shown in Fig. 12(b) there will be incidental amplitude modulation of the signal. It is expected this can be significantly decreased as film epitaxy improves (allowing greater use of kinetic inductance). The control line present in the electromagnetic structure will limit high frequency performance. The dependence of L_{out} on I_{bdy} can also be used for phase shifting (eliminating the need for a control line) at the expense of increased incidental amplitude modulation and nonlinear behavior.

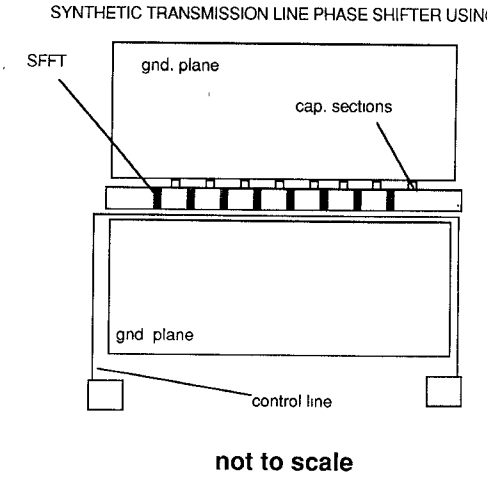

Fig. 11. Quasi-distributed phase shifter using the SFFT. The variable output inductance of the SFFT is used to change the phase velocity of the line.

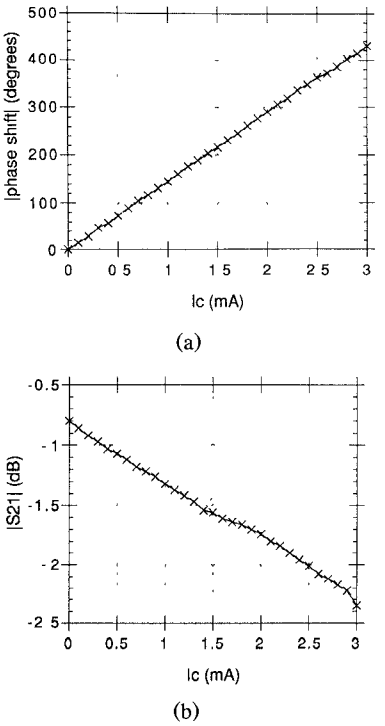

Fig. 12. Phase shift (a) and insertion loss (b) at 5.0 GHz of the YBaCuO phase shifter of Fig. 9 as a function of control current.

A Brief Comparison to Other Devices

At the present level of performance, the SFFT does not offer obvious advantages over HEMT's and HBTs in terms of noise, gain or power. Bandwidth appears to be a significant advantage in that we have used a device with 3 μm feature size at 40 GHz successfully; theoretically with 0.5 μm feature size operation at over 150 GHz is possible (based on the limiting event being the transit time constant). Also for high bandwidth applications, the distributed amplifier structure is more of a natural for the SFFT than for its conventional counterparts in that it is nearly unilateral. Based on rudimentary calculations, the noise performance will not significantly degrade from the 2–3 dB range to over 100 GHz, if that holds true another potential advantage emerges. Aside from some of the useful nonlinearities mentioned above, this high speed device has impedance levels that are very attractive for a small but increasing number of applications that need active impedance conversion not easily done with conventional electronics. These include transitions from Josephson circuitry or far-IR detectors (which prefer to drive low impedance loads) to high impedance processing electronics.

Conclusion

We have presented *S*-parameter measurements of a superconducting flux flow transistor. They indicate that a large amount of power gain is available, but significant matching must be employed. An example has been given

showing an amplifier with over 13 dB gain and a bandwidth of roughly 1 GHz at a center frequency of 4 GHz. Multistage and distributed structures are currently being investigated. The performance of a synthetic transmission line phase shifter using SFFTs has also been shown (2π of continuous phase shift available with insertion loss < 2.1 dB). As shown elsewhere, other applications including active impedance convertors [3] and mixers [5] have been successfully demonstrated as well.

Acknowledgment

The authors would like to thank Gert Hohenwarter of the University of Wisconsin-Madison and Parkview Works of Milton, WI for motivating some of the probing techniques and for useful discussions.

References

[1] G. K. G. Hohenwarter, J. S. Martens, D. P. McGinnis, J. B. Beyer, J. E. Nordman, and D. S. Ginley, "Single superconducting thin film devices for applications in high T_c materials circuits," *IEEE Trans. Magn.*, vol. MAG-25, pp. 954–956, Mar. 1989.

[2] J. S. Martens, G. K. G. Hohenwarter, J. B. Beyer, J. E. Nordman, and D. S. Ginley, "S parameter measurements on single superconducting thin-film three-terminal devices made of high-T_c and low T_c materials," *J. Appl. Phys.*, vol. 65, pp. 4057–4060, May 1989.

[3] J. S. Martens, D. S. Ginley, J. B. Beyer, J. E. Nordman, and G. K. G. Hohenwarter, "A Josephson junction to FET high speed line driver made of Tl-Ca-Ba-Cu-O," *IEEE Trans. Magn.*, vol. MAG-27, pp. 3284–3288, Mar. 1991.

[4] G. K. G. Hohenwarter, J. S. Martens, J. B. Beyer, and J. E. Nordman, "Resonant impedance matching of Abrikosov vortex-flow transistors," *IEEE Trans. Magn.*, vol. MAG-27, pp. 3297–3300, Mar. 1991.

[5] J. S. Martens, "The model and applications of a high frequency three terminal device made of high temperature superconductors," Ph.D. dissertation, University of Wisconsin-Madison, May 1990.

[6] K. K. Likharev, "Vortex motion and the Josephson effect in superconducting thin bridges," *Sov. Phys.-JETP*, vol. 34, pp. 906–912, Apr. 1972.

[7] T. Van Duzer and C. W. Turner, *Principles of Superconductive Devices and Circuits*. New York: Elsevier, 1981, Ch. 8.

[8] J. Pearl, "Current distribution in superconducting films carrying quantized fluxoids," *Appl. Phys. Lett.*, vol. 5, pp. 65–66, Jul. 1964.

[9] D. S. Ginley, J. F. Kwak, E. L. Venturini, B. Morosin, and R. J. Baughman, "Morphology control and high critical currents in superconducting thin films in the Tl-Ca-Ba-Cu-O system," *Physica C*, vol. 160, pp. 42–48, Oct. 1989.

[10] M. P. Siegal, J. M. Phillips, Y. F. Hsieh, and J. H. Marshall, "Growth of epitaxial $Ba_2YCu_3O_{7-x}$ films on $LaAlO_3$ (001)," *Physica C*, vol. 172, pp. 282–286, Dec. 1990.

[11] D. J. Carlson, M. P. Siegal, J. M. Phillips, T. H. Tiefel, and J. H. Marshall, "Stoichiometric effects in epitaxial $Ba_{2-x}Y_{1-y}Cu_{3-z}O_{7-\delta}$ thin films on $LaAlO_3$ (100)," *J. Mater. Res.*, vol. 5, pp. 2797–2801, Dec. 1990.

[12] M. P. Siegal, J. M. Phillips, R. B. van Dover, T. H. Tiefel, and J. H. Marshall, "Optimization of annealing parameters for the growth of epitaxial $Ba_2YCu_3O_{7-x}$ films on $LaAlO_3$ (001)," *J. Appl. Phys.*, vol. 68, pp. 6353–6360, Dec. 1990.

[13] T. Van Duzer and C. W. Turner, *Principles of Superconductive Devices and Circuits*. New York: Elsevier, 1981, ch. 3.

[14] "On-wafer measurements using the HP 8510 network analyzer and Cascade Microtech wafer probes," Hewlett Packard, Product Note 8510-6, 1986.

[15] G. Gonzalez, *Microwave Transistor Amplifiers*. Englewood Cliffs, NJ: Prentice-Hall, 1984, Ch. 3.

[16] J. S. Martens, J. B. Beyer, J. E. Nordman, G. K. G. Hohenwarter, and D. S. Ginley, "A superconducting single film device oscillator made of high T_c and low T_c materials," in *Proc. Int. IEEE MTT-S Symp.*, June 1989, pp. 443–446.

[17] J. S. Martens, V. M. Hietala, T. E. Zipperian, D. S. Ginley, and C. P. Tigges, "The superconducting flux flow transistor: models and circuit applications," in *Rec. IC SQUID*, Berlin, June 20, 1991.

[18] J. S. Martens, D. S. Ginley, T. E. Zipperian, V. M. Hietala, and C. P. Tigges, "Novel applications of Tl-Ca-Ba-Cu-O thin films to active and passive high frequency devices," in *Rec. Int. Symp. Superconductivity*, Sendai, Japan, Nov. 1990.

J. S. Martens received the B.S.E.E., M.S.E.E., and Ph.D. degrees in electrical engineering from the University of Wisconsin-Madison in 1986, 1988, and 1990 respectively.

Since 1990, he has been employed with Sandia National Laboratories, Albuquerque, NM. His current research interests are HTS and LTS microwave superconducting devices (both flux and Josephson based) and the millimeter-wave characterization of materials. He is a member of Sigma Xi.

Vincent M. Hietala (S'85–M'88) was born in Virginia, MN, on September 18, 1961. He received the B.S.E.E. With High Distinction, M.S.E.E., and Ph.D. degrees in electrical engineering from the University of Minnesota, Minneapolis, in 1983, 1987, and 1988, respectively.

In 1988, he was with Honeywell's Sensors and Signal Processing Laboratory, Bloomington, MN, where he worked as a Research Scientist on modeling optical waveguides and on the development of high speed optical data links. Since 1988 he has been a Staff Member in the compound-semiconductor device research group at Sandia National Laboratories, Albuquerque, NM. His current research activities include the development of high-speed devices and microwave/millimeter wave material characterization techniques. Dr. Hietala's research interests also include the application of lightwave technology to microwave systems.

Thomas E. Zipperian (S'71–M'80), was born in Helena, MT, on October 13, 1953. He received the B.S. degree in electrical engineering from Montana State University, Bozeman, in 1975 and the M.S. and Ph.D. degrees in electrical engineering from the University of Minnesota, Minneapolis, in 1978 and 1980, respectively.

In August of 1980, he joined Sandia National Laboratories, Albuquerque, NM. Since that time he has been engaged in research on a variety of physics, materials, and device topics in compound semiconductor technology. Subjects specifically of interest included studies in strained-layer superlattice and strained quantum well materials systems. At present, he continues studies in compound semiconductor areas as well as initiating new materials and device projects in thallium-based high-temperature superconducting thin films.

Dr. Zipperian is a member of Tau Beta Pi and the American Vacuum Society.

D. S. Ginley received the B.S. in mineral engineering chemistry from the Colorado School of Mines Golden, in 1972, and the Ph.D. in inorganic chemistry from the Massachusetts Institute of Technology, Cambridge, in 1976.

Since 1976, he has been employed by Sandia National Laboratories, Albuquerque, NM, where he currently is the Supervisor of an Advanced Materials Division. His research interests are in the materials growth

and processing of high temperature superconductors and compound semiconductors. He has approximately 200 publications and six patents.

Chris P. Tigges was born in Colorado in 1960. He received the B.S. degree in physics from Montana State University, Bozeman, in 1983, and the M.S., M.Phil., and Ph.D. degrees in applied physics from Yale University, New Haven, CT, in 1985, 1986, 1987, respectively.

From 1988–1990 he was a Postdoctoral Fellow and is presently a member of Technical Staff at Sandia National Laboratories, Albuquerque, NM, where he is engaged in experimental research in high temperature superconductivity and in computational simulations of III-V compound semiconductor device structures.

Julia M. Phillips received the B.S. degree in physics from the College of William and Mary, Williamsburg, VA, in 1976 and the Ph.D. in applied physics from Yale University, New Haven, CT, in 1981.

In 1981 she joined AT&T Bell Laboratories as a member of the Technical Staff. In 1988 she became the Supervisor of the Thin Film Research Group. Her interests include the growth and properties of epitaxial thin films and the relationships between film structure and other properties. She has authored or co-authored over 80 publications.